



Contents lists available at ScienceDirect

Transportation Research Part C

journal homepage: www.elsevier.com/locate/trc



Automated flight planning of high-density urban air mobility

Hualong Tang ^a, Yu Zhang ^{a,*}, Vahid Mohmoodian ^b, Hadi Charkhgard ^b

^a Department of Civil and Environmental Engineering, University of South Florida, USA

^b Department of Industry and Management Science Engineering, University of South Florida, USA



ARTICLE INFO

Keywords:

Conflict-free 4D trajectory planning
Air traffic management
Electric vertical takeoff and landing (eVTOL)
Aerodrome
Provider of service for UAM (PSU)

ABSTRACT

Advanced Air Mobility (AAM) is an emerging concept for transporting people and cargo in urban, rural, regional, and interregional settings using revolutionary new aircraft. Urban Air Mobility (UAM), a part of AAM, focused on transport passengers in low-altitude urban airspace, has attracted extensive attention among industry, government, academia, and the public. Compared to existing commercial flights, AAM operations are expected to be at higher density; thus, an AAM system needs to be scalable, safe, and autonomous. Third-party service providers are recommended for offering air traffic management and information sharing services given the anticipated high density of UAM operations. To this end, we propose an Automated Flight Planning System (AFPS) that could be employed by such service providers. In the AFPS, a Low-Altitude Airspace Management System (LAMS) is proposed to automatically generate a route network with the capability of avoiding obstacles and obstructions in low-altitude airspace. The main components of this tool are the generation of a 3D map with LiDAR data, construction of a nodal network based on the map by using the visibility graph method, and initiation of 3D shortest paths. Given the requests of flight operations, i.e., origin, destination, departure time, the Low-Altitude Traffic Management System (LTMS) will design pre-departure conflict-free 4D trajectories and provide flexibilities of en-route maneuvering by taking system cost and equity among operators into consideration. In this study, a flight-level assignment strategy is proposed to solve the trajectory deconfliction problem in LTMS. In addition, a Nash Social Welfare Program (NSWP) is introduced to maintain fairness among different operators if the service is provided to multiple operators of UAM. A case study of the Tampa Bay area in Florida is used to demonstrate the operability of the proposed AFPS, and animations are built to visualize the optimized conflict-free operations of UAM in the study area.

1. Introduction

UAM refers to a safe and efficient air transportation system that uses transformative new airborne technology, manned and unmanned, to move people and goods in a metropolitan area (Thippavong et al. 2018). UAM is a subset of AAM, which is a broader term that also covers rural areas and intercity travels (NASEM 2020). A wide range of envisioned AAM operations could include, but are not limited to, commercial transport and air taxi services; reconnaissance, surveillance, and inspection; shipping and delivery; geographic mapping; and search and rescue. The concept of UAM was practiced as early as the 1950 s with commercial helicopter services in Los Angeles but later disappeared in the early 1970 s, but with emerging technologies in electric propulsion, electronics, computer systems,

* Corresponding author at: 4202 E. Fowler Ave. ENB118, Tampa, FL 33620, USA.

E-mail address: yuzhang@usf.edu (Y. Zhang).

navigation, and sensing, AAM/UAM is expected to provide services with safety, efficiency, low noise, and reliability in areas not served or underserved by current air transportation modes. It is expected that AAM will exploit underused low-altitude urban airspace to alleviate congestion on the ground to some extent by offering an alternative to potential users and postponing large expenditures on expanding ground transportation infrastructures for accommodating continuously-growing travel demand.

Tremendously increasing interest by the industry and the public in Urban Air Mobility (UAM) and Advanced Air Mobility (AAM) has been observed over the past few years; a market of \$1.5 trillion by 2040 was forecasted by Morgan Stanley (Morgan Stanley 2019). Recently, the National Academies of Sciences, Engineering, and Medicine (NASEM) published a blueprint for AAM, and the Federal Aviation Administration (FAA) NextGen Office also published UAM Concept of Operations v1.0 (hereafter referred to FAA UAM ConOps). In Europe, the SESAR Joint Undertaking has launched large demonstrator projects aiming at extending the U-space ConOps for drones by the addition of UAM (SESAR Joint Undertaking 2021).

Although the benefits of AAM are foreseeable, challenges and barriers need to be addressed to realize successful operations, including air vehicle technologies such as safety, batteries, propulsion, noise, and energy consumption, and how AAM/UAM can be integrated into the existing national airspace system and whether/what management systems need to be developed to serve anticipated future high-density AAM/UAM operations. The legacy ATM system is heavily dependent on human operators, which will not be able to accommodate the density of operations AAM expects. Also, current communication, navigation, and surveillance (CNS) technologies, airspace structure, and procedures over low-altitude urban airspace are designed for helicopters and General Aviation (GA) aircraft but not high-density AAM operations because: 1) the separation of two aircraft flying under visual flight rules (VFR) relies on the “see and avoid” principle, and such system will not work for high-density AAM operations; 2) verbal communication would be very challenging for hosting high-density AAM operations (Vascik, Balakrishnan, and Hansman 2018); and 3) the prevailing surveillance, automatic dependent surveillance-broadcast (ADS-B), may have issues for dense airspace (Guterres et al. 2017). As the legacy ATM system is not suitable for future AAM operations and realizing the unique challenges of UAM, this paper is focused on designing a flight planning system that can plan conflict-free 4D trajectories for UAM flights operating in high-density traffic and meanwhile considering the fairness among different UAM operators.

FAA UAM ConOps V1.0 envisions a shared responsibility for traffic and airspace management across service providers, aircraft operators, and other entities without increased workload to Air Traffic Control (ATC) (NextGen 2020). This document suggests the use of commercial service providers, including Providers of Services for UAM (PSU) and Supplemental Data Service Providers, rather than existing ATC to handle the needs of UAM operations. NASA defined UAM maturity levels (UMLs) and is seeking to expand the unmanned aircraft system (UAS) traffic management (UTM) system to UAM and enable UAM flights to interact with both UTM and ATM (NASA 2020). The UAS service suppliers (USSs) proposed in NASA's framework can also be looked at as a PSU and vice versa. SESAR's Demonstration of Multiple U-space Suppliers (DOMUS) demonstrated the feasibility of having multiple U-space service providers interacting with several drone operators to conduct strategic and tactical conflict resolution in real-time (SESAR Joint Undertaking 2020). Meanwhile, corporations that plan to offer high-density AAM services for goods delivery and passenger transportation in the future are seeking ways to manage their fleet and operations by developing their own dispatching centers covering PSU functions.

UAM operating in low altitude urban airspace may encounter many conflicts with buildings, obstructions, and restricted airspaces. Some studies have suggested the use of existing helicopter routes to construct the route network in initial UAM operations (NextGen 2020). FAA UAM ConOps V1.0 suggests a corridor concept to support UAM operations. Nevertheless, a route network based on existing helicopter routes or corridor concepts suggested by FAA is limited and can only serve early-stage low-density UAM operations. With the increasing number of vertiports and high-density operations (UML levels of 4 and above) of future UAM, the challenge exists in how to construct a route network that is capable of enabling safe and efficient flight trajectories.

Two crucial questions need to be answered when planning trajectories in low-altitude environments with high-density operations. The first is how route networks should be constructed and the second is how conflicts should be resolved. Thus, in this study, we developed an Automated Flight Planning System (AFPS) that could enable service providers for high-density UAM operations, i.e. UMLs 4 and above according to NASA classification (NASA 2020). In the AFPS, a Low-Altitude Airspace Management System (LAMS) is proposed to automatically generate a route network with the capability of avoiding obstacles and obstructions in low-altitude airspace. The main components of this tool are the generation of a 3D map with LiDAR data, construction of a nodal network based on the map by using the visibility graph method, and initiation of 3D shortest paths. Given the requests of flight operations, i.e., origin, destination, and departure time, the Low-Altitude Traffic Management System (LTMS) will design pre-departure conflict-free 4D trajectories and leaves flexibilities of en-route maneuvering by taking system cost and equity among operators into consideration. In this study, a flight level assignment strategy is proposed to solve the trajectory deconfliction problem in LTMS. In addition, a Nash Social Welfare Program (NSWP) is applied to maintain fairness among different operators if the service is provided to multiple operators. A case study of the Tampa Bay area in Florida is used to demonstrate the operability of the proposed AFPS, and animations are built to visualize the optimized conflict-free operations of UAM in the study area.

Traditional flight planning determines the route, flying altitude, and speed, and the minimum necessary fuel on board. For UAM service with electric vertical takeoff and landing (eVTOL) vehicles, monitoring the battery level and determining the charging schedule of eVTOLs is more of tactical operational decisions dependent on the number of charging pads at each vertiport and flight operational scheduling (distance between origin and destination of succeeding flight). We use “flight planning” instead of “trajectory planning” in our study, focusing on generating conflict-free 4D trajectories of high-density UAM operations and distinguishing it from trajectory planning in the existing literature that focused on designing optimal fuel-efficient trajectory of single eVTOL considering the dynamics of the vehicle.

The remainder of this paper is organized as follows. Section 2 summarizes an overview of related studies in airspace design, conflict detection, trajectory deconfliction, and flight equity. Section 3 presents the research approach of developing the AFPS, consisting of

two subsystems – a Low-Altitude Airspace Management System (LAMS) and a Low-Altitude Traffic Management System (LTMS). Section 4 introduces the case study of the Tampa Bay area and the results of applying the proposed AFPS. Finally, Section 5 summarizes the research and discusses the limitations of the current study and future research directions.

2. Literature review

2.1. Airspace design

Although the current air transportation system is a nodal network, its legacy static routing structure limits direct connectivity between origin and destination points, which makes it a relatively sparse network and challenging for organizing rerouting during irregular operations. High-density AAM desires a dense nodal network, which could ensure the utilization of airspace capacity and provide more point-to-point direct connectivity between origins and destinations (NASAM 2020). Much literature has studied the relationship between airspace design and capacity, safety, and efficiency of the airspace and tried to improve and optimize airspace use for commercial flight traffic. There also has been debate on if the future integrated airspace, with advanced automated and autonomous technologies, should be structured or free-flight. Several studies have argued that structured airspace is the essential cornerstone for accommodating high-density traffic (Prevot et al. 2003; Andrews, Welch, and Erzberger 2006; Hunter, Wei, and Wargo (2019) pointed out that structured airspace is a key component to the sUAS separation assurance problem, as it can greatly reduce the airspace complexity and lessen the ATC workload; more importantly, it can facilitate situational awareness and simplify alert boundaries and conflict detection by concentrating traffic. On the other hand, researchers argued that free-flight is a better airspace design concept than structured airspace because it spreads the traffic over the airspace so as to reduce the number of potential conflicts; flights can fly user-preferred routes to save fuel, and each aircraft is responsible for its own separation assurance, thus alleviating the flow constraints and structure to handle a higher traffic density (Jardin 2005; Hoekstra, Van Gent, and Ruigrok 2002; Krozel, Peters, and Bilmoria 2000). Sunil et al. (2015) further compared the influence of four different airspace structures—Full Mix (free-flight), Layers, Zones, and Tubes—on capacity, safety, and efficiency for high-density airspace. The simulation results indicated that a layered concept is optimal in terms of balancing capacity, safety, and efficiency.

FAA UAM ConOps proposed the concept of a UAM corridor, which is designated airspace connecting UAM aerodromes in which all aircraft (UAM, commercial, UTM) must comply with UAM specific rules, procedures, and performance requirements regardless of airspace class (NextGEN 2020). The aircraft conform to corresponding ATM or UTM rules when outside the corridor, and the corridor can also expand its structure by adding “tracks” vertically to meet future operation increases. The corridor structure evolves from initial helicopter routing to UAM-specific corridors to accommodate early-stage UAM services. To deal with the interaction of UAM with manned aircraft, a geo-fenced corridor is defined for the approach and departure of commercial flights around the airport runway where UAM is forbidden to enter into the corridor (William, Cotton, and Wing 2018).

Arrival and departure procedures of commercial flights need to consider inevitable obstructions near the airport, e.g., mountains, tall buildings existing due to historical reasons, etc. For UAM using low-altitude airspace in metropolitan areas, potential conflicts coming from the aircraft interacting with buildings, obstructions, and terrain in the urban airspace need to be considered in the airspace design process. However, most existing studies tackled conflict resolution in the tactical phase of traffic management but did not touch airspace management. A few studies, such as Tan and Wang (2019), proposed an urban airspace design for UAS. In that study, the airspace was configured with multiple players of air-blocks and nodes, and links were removed if conflicting with buildings. Although a route network built in this airspace can successfully avoid buildings, the generated trajectories have zig-zag shapes that are excessively indirect and not efficient.

In computational geometry and robot motion planning, a visibility graph has been used often to find the shortest path among a set of polygonal obstacles in the Euclidean plane (de Berg et al. 2000). Unlike grid-based airspace structures that airspace is discretized into small cubes with a large number of nodes and edges connecting them. The visibility graph tends to have much fewer nodes and edges. Nodes in the visibility graph consist of origin, destination, and polygonal vertices. The edges in the visibility graph connect the origins, destinations, and vertices of the polygons if they are not blocked by the polygons. A good property of the visibility graph is that the shortest path of any origin and destination (OD) pair is among all the paths consisting of edges on the graph. In other words, by applying a shortest path algorithm, the shortest path of any OD pair can be found based on the network constructed by a visibility graph.

2.2. Conflict detection

One criterion for distinguishing conflict detection methods is projection methods of the future state of aircraft. How the future state is estimated determines the reliability of conflict detection. Kuchar and Yang (2000) identified three extrapolation methods—nominal, worst case, and probabilistic. Conflict detection can be further classified as space-based, time-based, and space-time-based methods. Space-based methods use the distance between any two trajectory points at a time as the criterion to determine if they violate the minimum separation requirement in the horizontal or vertical plane (Barnier and Allignol 2011; Rey et al., 2012). Time-based methods use the time interval between any two aircraft passing the intersection point as the criterion to determine if they violate the minimum time separation determined by the velocity and intersection angle of the two aircraft (Vela et al. 2009; Tan and Wang 2019). Space-time-based methods discretize the time; at each time step, space is discretized into grids (Islami, Chaimatanan, and Delahaye 2016) for detecting if there are any conflicts.

2.3. Trajectory deconfliction

Trajectory deconfliction methods can be generally classified as a centralized and decentralized approach. The key difference between these two approaches is whether there is a central utility to solve all conflicts or if each aircraft is responsible for its separation assurance with other aircraft. The centralized approach could be used for both strategic and tactical deconfliction, and a decentralized approach is used for tactical deconfliction only. In the FAA NextGen ConOps, separation in the corridor is maintained primarily by strategic deconfliction provided by service providers, whereas it is the UAM operators' responsibility to take tactical deconfliction. U-space may require UAS and UAM operators operating in high-density environments to be equipped with Detect and Avoid (DAA)/collision avoidance technologies to ensure separation provision. The service provider will support strategic and tactical deconfliction.

Centralized methods are typically modeled as an optimal control/optimization problem trying to find the global optimum under conflict-free constraints (Durand et al. n.d.; Frazzoli et al. 1999; Durand et al. n.d.). Some studies developed approximate models of aircraft dynamics using only linear constraints (Richards and How n.d.; Schouwenaars et al. n.d.); in other studies, nonlinear programming (NLP) was used to address the flyability issue by allowing the use of dynamic aircraft models at any desired level of detail (Raghunathan et al. 2004). In addition, some studies used mixed-integer linear programming (MILP) and NLP to solve the aircraft conflict problem with different maneuvers (heading, speed, altitude), spaces (2D and 3D), and objectives (flying time, energy consumption, safety) (Vela et al. 2009; Alonso-Ayuso, Escudero, and Martín-Campo 2016). Deconfliction methods in a strategic manner can be classified into several approaches based on the degree of freedom. Flight level assignment uses the spatial dimension to resolve conflicts (Barnier and Brisset 2002; Nace et al. 2003). Ground holding uses the temporal dimension to adjust the departure time to resolve conflicts. Also, speed control can be used to resolve conflicts (Courchelle et al. 2017). The combination of different methods noted can also be found in the literature (Barnier and Allignol 2011; Islami, Chaimatanan, and Delahaye 2016). In the arena of UAM, Zhu and Wei (2019) proposed a linear programming model to plan the conflict-free trajectory before departure with collision resolutions of rerouting and departure delay. However, the conflict-free trajectory planning was only for one cruise level; obstructions affecting flyable airspace were not considered.

On the other hand, decentralized approaches have been studied greatly, particularly under the concept of free flight for tactical conflict resolution, including methods inspired by physical laws (Sigurd and How 2003; Eby and Kelly III n.d.), geometric optimization (Allignol et al. 2016; Ho et al. 2019), and Markov Decision Process (MDP) (Bertram et al. 2021; Bertram and Wei 2020; Yang and Wei 2020). Bertram et al. (2021) formulated a strategic deconfliction problem for UAM as an MDP and used the FastMDP algorithm to solve it and generated conflict-free trajectories. Yang, Deng, and Wei (2019) formulated the collision avoidance problem similarly as an MDP and then solved it using an online algorithm Monte Carlo Tree Search (MCTS) among cooperative aircraft. The authors further considered communication constraints in the model by proposing two communication strategies, air-to-ground and air-to-air communications (Yang and Wei 2020). Although these decentralized approaches can avoid potential conflicts when the proposed algorithm performs efficiently and are applicable for real-time operation, one of the main issues is that the global optimum cannot be guaranteed. For example, there still exist a few conflicts in the noted MDP method (Yang, Deng, and Wei 2019), and the results showed a conflict probability of around 0.23% in the case of air-to-ground communication (Yang and Wei 2020).

2.4. Flight equity

U-space underscored the importance of investigating the impact of fairness principles on the decision-making process in order to develop scalable advanced U-space services (U3 & U4) (SESAR Undertaking, 2019). In air transportation, several metrics or criteria have been developed and applied to ensure equity/fairness among flights and operators. For example, a first-scheduled-first-served (FSFS) priority discipline has been applied in the rationing by schedule (RBS) under the ground delay program (GDP) (Lulli and Odoni 2007). To contain large deviations from the nominal sequence, constrained position shifting (CPS), i.e., restricting the maximal position shifting in reordering or average flight position deviation, has been used to maintain equity while solving the aircraft arrival sequencing and scheduling (ASS) problem (Balakrishnan and Chandran 2007; Jacquillat and Vaze 2018). Other disciplines such as constraining average or maximum flight delays have also been proposed in the literature (Barnhart et al. 2012). However, these methods do not necessarily reflect true equity among players in terms of the benefits they receive from using the service of the AAM/UAM service provider. Nash Social Welfare (NSW), introduced by Nash (1950) as a solution for bargaining problems, was used to model fairness in terms of the benefit each play receives. NSW chooses the solution that maximizes the product of benefits of players, which makes it superior to other measures such as utilitarian social welfare and egalitarian social welfare in terms of fairness (Branzei et al., 2017; Nguyen et al. 2014).

2.5. Literature summary

Although a corridor structure proposed by FAA UAM ConOps is feasible for initial operations, with the increasing number of vertiports and operation density, a nodal network is foreseen as suitable for UAM. It will be more complex than the current nodal network for commercial flight operations in terms of the number of nodes and combination static and flexible nodes. Also, regarding the debate of structured airspace vs. a free-flight concept, according to existing studies, a layer structure in between could work the best by balancing safety and efficiency. Although there have been studies comparing airspace design for AAM through simulation and performance comparison, they lack general tools for constructing flyable airspace in urban and metropolitan areas with obstructions (high buildings, power towers, etc.) for high-density UAM operations. For a few studies that designed urban airspace for UAVs, most of them used a grid-based method that discretizes airspace into small cubes. The shortcoming of such a method is for being able to plan a

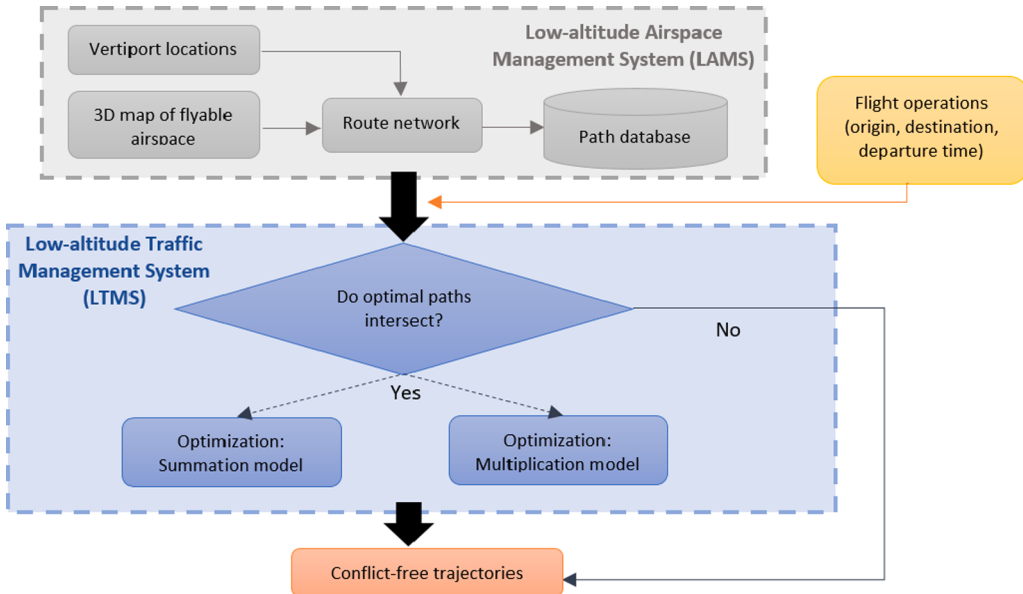


Fig. 1. Workflow of AFPS.

path as close as the shortest path, it requires a high resolution of airspace discretization, which inevitably increases the numbers of nodes and edges and thus the route network complexity. For high-density operations in a metropolitan area, a grid-based airspace design would be computationally expensive to find the shortest paths and resolve conflicts. The visibility graph method can create a nodal network with much fewer nodes and edges.

Based on the nodal network, how to design an airspace route network for service providers that enables optimal pathfinding and supports conflict resolution with efficiency and safety is needed for UAM. This route network should be able to avoid obstacles and obstructions in low-altitude airspace and find the shortest path from origin to destination. The existing literature lacks answers to this need.

From both FAA UAM ConOps and U-space's envisions, service providers are expected to support the pre-departure strategic conflict resolution and some of the tactical resolution, while most tactical and real-time conflict resolution/collision avoidance will be conducted by onboard DAA/collision avoidance technologies. Although a number of studies have paid attention to decentralized deconfliction approaches for UAS and UAM, there lacks research in centralized approaches that can guarantee pre-departure conflict-free trajectories for high-density operations of UAM.

One service provider may offer its services to multiple UAM operators. Fairness will be a key factor for operators to be willing to use the services. The rules used for solving current traffic flow management problems are not suitable for dealing with the equity/fairness of UAM operations. Based on the literature review, NSW that considers the benefits received by operators for using the service is a better measurement. Some co-authors' recent work developed a Nash Social Welfare Program (NSWP) that can maximize the product of users' benefits. Such a method can be applied to address equity issues in the traffic flow management of UAM.

To fill the aforementioned research gaps in airspace route network design, conflict resolution, and equity, we propose an Automated Flight Planning System (AFPS) that enables service providers to generate nodal networks avoiding obstacles and obstructions in low altitude urban airspace and generate pre-departure, conflict-free trajectories while considering equity of multiple UAM operators. The nodal network is a near-free airspace structure with layers that allow possible point-to-point routing for UAM flights. The visibility graph, together with the shortest path algorithm, is used to construct this route network that can generate the shortest paths while avoiding obstacles. We opted for a centralized deconfliction method by assigning flights at different layers to avoid potential conflicts. More freedoms, such as departure replacement and speed control, are considered in our ongoing study but are not included in this paper. NSW is used to model the equity among operators to better capture the benefits received from using a service provider.

3. Research approach

The proposed AFPS consists of two subsystems (see Fig. 1)—a Low-Altitude Airspace Management System (LAMS) and a Low-Altitude Traffic Management System (LTMS). LAMS starts by generating a 3D map of the study region and defining flyable airspace by indicating obstructions. Given this map and vertiport (or called aerodrome in FAA UAM Conops V1.0) locations (determined from the network design and demand estimation study in Wu and Zhang, 2021), the LAMS generates a 3D route network for all vertiport pairs and identifies the shortest paths of vertiport pairs flying at each flight level by using a visibility graph method to avoid obstructions. The information from these shortest paths is stored in a database, including coordinates of the crossing points of these paths. Given the requests of flight operations (departure vertiport, arrival vertiport, desired departure time), the LTMS first looks up the

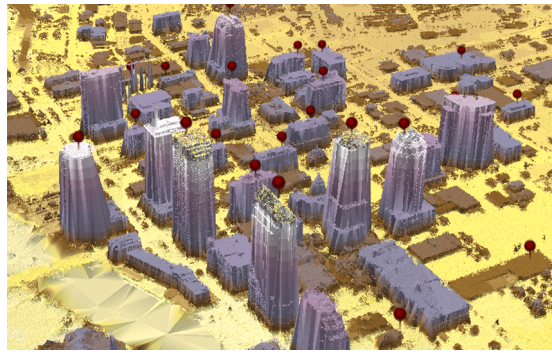


Fig. 2. 3D map of Tampa downtown based on LiDAR data.

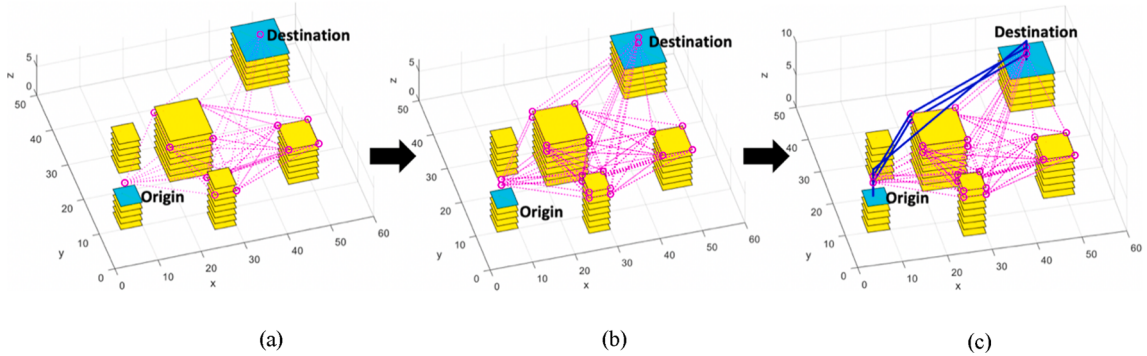


Fig. 3. Workflow of generating route network in LAMS.

optimal shortest path of each vertiport pair, i.e., the shortest path consuming the least energy after considering aircraft dynamics for these operations. The LTMS then looks up the database to see if any optimal shortest paths will cross after considering the departure time of the flights (i.e., 4D trajectory). If not, all flights can take their optimal routes and depart at their desired time. If the answer is yes, the mathematical programming in LTMS will be solved to obtain conflict-free trajectories of all flights by minimizing system-wide generalized cost and ensuring equity. It should be noted that we develop two models in LTMS, the summation model and the multiplication model. Users can choose either model in LTMS based on their own preference. That's why dashed lines are connected to them. LAMS and LTMS are elaborated in the following subsections.

3.1. Low-altitude airspace management system (LAMS)

Most AAM operations, including UAM, will be conducted in the low-altitude airspace of metropolitan areas. According to FAA regulations, for small UAS (less than 55 lbs), the maximum allowable altitude is 400 ft above the ground, higher if the UAS remains within 400 ft of a structure. Also, the maximum speed of sUAS is restricted to no more than 100 mph (87 knots) (FAA 2020). Two major use cases of AAM will be goods and passenger transportation. Goods transportation includes intercity and inter-distribution-center by using relatively large aircraft and local drone delivery for small packages within short distances. For passenger transportation, the current prevailing VTOL design has a seating capacity of 2–6 for both air shuttle and air taxi purposes. There has been discussion on VTOLs with larger capacity that could work as “bus in the air”; however, no prototype has been built and no market studies have been conducted to demonstrate potential economic viability. In addition, when technology and regulation mature, market penetration of personally-owned VTOLs could increase. More backyard takeoff and landing will be realized, which will bring the maturity of UAM to another level.

Future AAM operations require high accuracy and reliable navigation. Although there are technology challenges, it is believed that they will not be limiting factors. For instance, there were concerns that UAS and UAM operations would be impacted by “urban canyons,” as GPS signals might be blocked by tall structures in an urban area. NASA conducted a series of experiments to test the performance of sUAS GPS navigation in downtown Corpus Christi, Texas, and preliminary results showed that there was sufficient accuracy and reception of GPS navigation satellites to support sUAS operation in an urban canyon (Logan et al. 2020).

Thus, for this study, we propose an airspace design by having airspace 400 ft and below used for drone delivery and 500–1400 ft for urban, metropolitan, and intercity cargo and passenger transportation. We focus on UAM using a certain number of vertiports (tens to hundreds, but not door-to-door, i.e. UML 4 and above) and en-route 500–1400 ft airspace. The airspace is configured with a number of layers to give it flexibility in conducting obstruction avoidance and trajectory deconfliction. Given this airspace concept, the rest of the

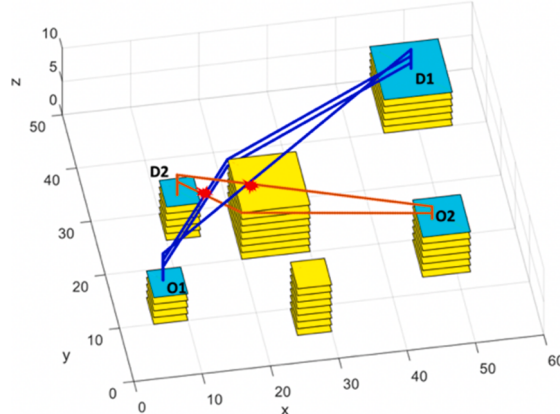


Fig. 4. Example of route intersecting.

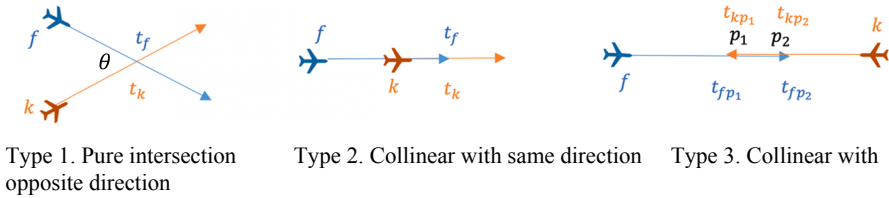


Fig. 5. Types of intersections.

workflow of LAMS is as follows:

1. Construct a 3D GIS map of the region based on geographic and LiDAR data. Flyable airspace is determined by the map and corresponding regulations. The LiDAR data points are shown in Fig. 2, with potential vertiports on top of the buildings.

2. Construct a visibility graph for each vertiport pair at each flight level (see Fig. 3(a)). To build up a nodal network, a visibility graph is used, in which a node represents the vertices of obstacles and an edge represents a connection between those nodes that are not blocked by the obstacles.

3. Obtain the shortest path of each vertiport pair at each flight level. Given the visibility graph generated at each flight level, the shortest path (3D trajectory) of any vertiport pair at each flight level can be obtained by applying a shortest path algorithm.

Fig. 3 illustrates an example of how a route network is generated. Based on LiDAR data, the obstacles shown as boxes are constructed in a 3D map at different flight levels, and a visibility graph is constructed given origin and destination vertiport locations. Fig. 3(a) shows a visibility graph (in magenta edges and nodes) constructed at one flight level between the origin and destination vertiports. Fig. 3(b) shows visibility graphs at different flight levels. Based on the visibility graphs, the shortest paths going through different flight levels are obtained. The blue lines in Fig. 3(c) show the three shortest paths as an example.

4. Pre-process all shortest paths, identify crossing coordinates, and store information in a database.

Fig. 4 gives an example of the shortest paths for two OD vertiport pairs (shown in blue and orange, respectively). The intersections of 3D trajectories at different flight levels can easily be seen. A database is created to store the shortest path at different levels and the information of intersections of 3D trajectories.

3.2. Low-altitude traffic management system (LTMS)

The LTMS is designed for detecting and resolving conflicts. The conflict detection method is explained, and two mathematical models with and without considering equity are introduced for conflict resolution, referred to as the summation model and the multiplication model, respectively.

3.2.1. Conflict detection

Given the request of flight operations (departure vertiport, arrival vertiport, desired departure time), without considering time dimension, LTMS first looks up the database generated by LAMS to see if the optimal shortest paths after considering energy consumption of different phases of eVTOL operations intersect with each other. If not, no further action is needed, and the flights can depart at their desired time and follow their optimal routes. This might occur at the early stages of UAM when the density of operations is low. Otherwise, LTMS generates 4D trajectories based on the 3D trajectories obtained in LAMS and eVTOL dynamics (takeoff, cruise, landing speeds) and checks again if 4D trajectories intersect with each other.

After considering departure time, there are three types of intersections for 4D trajectories—Type 1, pure intersection (intersection

$\text{angle}\theta > 0$; Type 2, collinear with the same direction; and Type 3, collinear with opposite direction, as illustrated in Fig. 5.

A conflict is a situation occurring when two or more aircraft violate the minimum lateral separation D^s . Given aircraft speeds, intersection angle, minimum lateral separation D^s , and linearly-extrapolated trajectories, the minimum temporal separation between aircraft at their intersecting point is given by (Vela, et al. 2009):

$$S_{fk} = \begin{cases} \frac{D^s}{v_f v_k |\sin(\theta_{fk})|} \sqrt{v_f^2 + v_k^2 - 2v_f v_k \cos(\theta_{fk})}, & \text{Type 1} \\ \frac{D^s}{v_a}, & \text{Type 2 or Type 3} \end{cases} \quad (1)$$

where v_f and v_k are the aircraft speeds of flight f and flight k respectively, θ_{fk} is their intersection angle, which is greater than zero for Type 1 intersection, D^s is the minimum lateral separation, and S_{fk} is the minimum temporal separation. For Type 2 and Type 3 intersections, S_{fk} is obtained by dividing the minimum separation D^s by average aircraft speed v_a .

Conflict detection is conducted by checking the interval between two aircraft crossing the intersecting point. If the interval is greater than the minimal temporal separation, then there is no conflict. Given S_{fk} is the minimum temporal separation between flight f and k and assuming they have the same speed, for Type 1 and Type 2 intersections, safety can be assured as long as the interval of the two aircraft crossing the intersection point is greater than the minimal temporal separation. The relationship is expressed in Equation (2):

$$|t_f - t_k| \geq S_{fk} \quad (2)$$

In the case of a Type 3 intersection, the ends of routes that potentially overlap need to be identified for detecting conflicts. The relationships in equation (4) are used to detect the conflict, and there will be no conflicts when either of the constraints is met. The first relationship ensures that flight f arrives at the first intersecting point p_1 later than the time flight k arrives at this point plus the minimal temporal separation S_{fk} . The second relationship ensures that flight k arrives at the second intersecting point p_2 later than the time flight f arrives at this point plus the minimum temporal separation S_{fk} .

$$\begin{aligned} t_{fp_1} &\geq t_{kp_1} + S_{fk} \text{ or} \\ t_{fp_2} + S_{fk} &\leq t_{kp_2} \end{aligned} \quad (3)$$

3.2.2. Mathematical model

If 4D trajectory conflicts are detected, mathematical models are proposed for determining conflict-free trajectories. Flight level assignment is used as the strategy to resolve conflicts. If multiple operators use the service, service providers need to ensure equity among the operators by not favoring any of them because of more operations or different patterns of operations. Thus, two models are proposed, one to minimize the summation of generalized cost of all flights (summation model) regardless of equity, and the other to minimize the product of each operator's benefit (multiplication model) considering equity amongst operators.

Consider a set of flights F operating in low altitude airspace that is divided into $|H|$ flight levels. The departure time is given for each flight $f \in F$. The available flight levels allowed for flight f is in set $L^f \subseteq H$ according to the departure and arrival vertiports. Suppose the en-route trajectories of flight f, k spatially intersect with each other on flight level h . Let P_h^{fk} denote the set of intersecting points from the two trajectories. These points can further be categorized as Type 1, Type 2, and Type 3 intersecting points. Let $P_h^{fk12} \subseteq P_h^{fk}$ denote the collection of Type 1 and Type 2 points and $P_h^{fk3} \subseteq P_h^{fk}$ denote the Type 3 points. Given flight speed and the distance from the origin to an intersecting point which is stored in the path database in LAMS, the crossing time of flight f passing the intersecting point can be obtained. The crossing time for flight f passing a Type 1 or Type 2 point is defined as t_{fp} , where $p \in P_h^{fk12}$. For a Type 3 intersection, there are two intersecting points, defined as t_{fp_1} and t_{fp_2} respectively, where $p_1 \in P_h^{fk3}$ and $p_2 \in P_h^{fk3}$. Below, we first describe the notation, summarizing the above set of parameters and describing the variables. This is followed by the mathematical formulation of the summation model and the multiplication model and explanations of all the expressions.

Parameters:

F : set of flights.

H : set of flight levels.

$L^f \subseteq H$: set of flight levels allowed for flight f .

$I_h^f \subseteq F$: set of flights that spatially intersects with flight f on level h .

$P_h^{fk} \in \mathbb{R}^2$: set of spatially intersecting points between flight f and flight k on level h .

$P_h^{fk12} \subseteq P_h^{fk}$: set of Type 1 and Type 2 intersecting points for $f, k \in F$ and $h \in H$.

$P_h^{fk3} \subseteq P_h^{fk}$: set of Type 3 intersecting points for $f, k \in F$ and $h \in H$.

C_f^h : flying cost of flight f taking level h .

t_{fp} : crossing time of flight f passing an intersecting point $p \in P_h^{fk12}$.

t_{fp_1} : crossing time of flight f passing the first intersecting point $p_1 \in P_h^{fk3}$.

t_{fp_2} : crossing time of flight f passing the second intersecting point $p_2 \in P_h^{fk3}$.

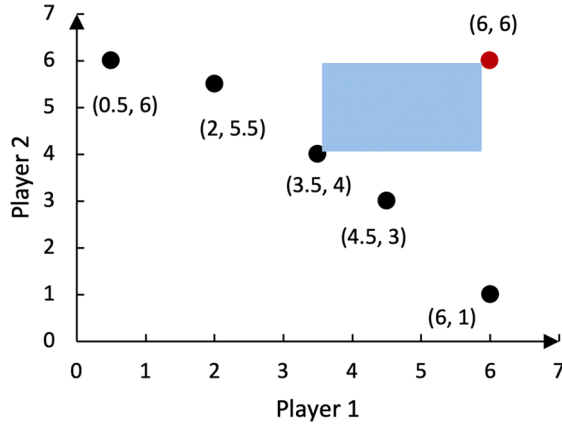


Fig. 6. Pareto-optimal point selected by NSW.

S_{fk} : the minimal temporal separation between flight f and k .

Variables:

$\phi_h^f \in \{0, 1\} : \phi_h^f = 1$, if flight f assigned to flight level h ; otherwise, $\phi_h^f = 0$.

$y_{fkhp} \in \{0, 1\} : y_{fkhp} = 1$, if the intersecting point p of flight f and k is Type 3 and satisfies the first relation in (3); $y_{fkhp} = 0$, If p is Type 3 intersection and satisfies the second relation in (3).

Summation model

$$\text{Min} \sum_{f \in F} \sum_{h \in L^f} C_f^h \phi_h^f \quad (4)$$

s.t.

1. Each flight assigned to one and only one flight level:

$$\sum_{h \in L^f} \phi_h^f = 1, \forall f \in F \quad (5)$$

2. Conflict resolution:

(1) For pure intersection and collinear with same direction:

$$|t_{fp} - t_{kp}| \geq S_{fk} + M(\phi_h^f + \phi_h^k - 2) \quad (6)$$

$$\forall f \in F, \forall k \in L^k, \forall p \in P_h^{fk12}, \forall h \in L^f \cap L^k$$

(2) For collinear with opposite direction:

$$y_{fkhp} (t_{fp_1} - t_{kp_1} - S_{fk}) \geq M(\phi_h^f + \phi_h^k - 2) \quad (7)$$

$$\forall f \in F, \forall k \in L^k, \forall p_1, p_2 \in P_h^{fk3}, \forall h \in L^f \cap L^k$$

$$(1 - y_{fkhp}) (t_{fp_2} - t_{kp_2} + S_{fk}) \leq M(2 - \phi_h^f - \phi_h^k) \quad (8)$$

$$\phi_h^f, \phi_h^k, y_{fkhp} \in \{0, 1\}$$

The summation model is formulated as an integer program with the objective of minimizing total flying cost. The objective function shown in Equation (4) sums the flying cost C_f^h of each flight f assigned to the flight level h . The decision variable ϕ_h^f determines which flight level flight f takes. Each flight is assigned to the one and only flight level expressed in Equation (6). Constraint (6) ensures that Types 1 and 2 conflicts will not occur in optimized solutions and constraints (7) and (8) for Type 3 conflicts. To resolve Type 3 opposite direction conflicts, constraint (8) ensures that flight f arrives at p_1 after the time flight k arrives at this intersection point plus their required minimal temporal separation S_{fk} . Constraint (8) ensures that flight k arrives at p_2 after the time flight f arrives at p_2 plus their required minimal temporal separation S_{fk} . y_{fkhp} is a binary variable to fulfill either constraint (7) or (8). Big M is used to represent a large enough constant in conflict resolution constraints.

The summation model optimizes the whole system, aiming only at minimizing total flying cost. If all flights belong to a single operator, the logic of the model can be justified. However, the summation model does not consider the equity among multiple op-

erators. Although the summation model can be reformulated as a multi-objective optimization program (MOOP) and by obtaining Pareto frontier, the tradeoff between the objectives of different operators can be balanced, computing the Pareto frontier can be expensive. Also, selecting a desirable Pareto-optimal solution from the frontier is subjective and challenging, which requires the decision-maker to have comprehensive knowledge of the problem. Furthermore, if such non-convex multi-objective problem is modeled as a single-objective optimization problem (SOP) in a weighted sum form for considering the equity among different operators, the optimal point would be selected from endpoints but not points in the middle (unsupported Pareto-optimal points) of the Pareto frontier (Charkhgard, Esmaeilbeigi, and Charkhgard 2020). For example, as shown in Fig. 6 where there are two players/operators and five Pareto-optimal points, if the problem is modeled as SOP in a weighted sum form, an endpoint, either point (0.5, 6) or point (6, 1) for any possible weights of w_1 and w_2 will return as the optimal solution but none of the three middle points will be obtained because they are unsupported Pareto-optimal points. For operators with different frequency or patterns of operation, it is unclear who will be favored by the system because any endpoint could be selected but it is clear that the optimal solution from the summation model is unlikely to be a fair point that balances the objectives of different operators and ensures the fairness amongst them.

Multiplication model

Thus, the NSWP was used in this study to overcome the weaknesses of the summation model; it can reduce computation time significantly and it returns a single Pareto-optimal solution when solved to optimality. The NSWP does not ignore unsupported Pareto-optimal points and ensures a balanced and equitable resource assignment among competing players (Charkhgard, Esmaeilbeigi, and Charkhgard 2020).

The general form of NSWP for minimizing its objective function is shown in Equation (9). We assume there are n number of players and $|S| = n$. Each player $i \in S$ has an objective function g_i . $\mathcal{X} \subseteq \mathbb{R}^n$ is the set of feasible solutions and $d \in \mathbb{R}^n$ is the reference point, which is defined as the payoff of each player under no coalition in game theory. $w : (w_1, \dots, w_n)$ is a vector of weights for players concerning their powers. $d_i - g_i(x)$ represents the benefit player i can obtain compared to the reference point. The objective function is to maximize the product of each player's benefit.

$$\begin{aligned} & \text{Max} \prod_{i \in S} (d_i - g_i(x))^{w_i} \\ & \text{s.t. } x \in \mathcal{X} \\ & g_i(x) \leq d_i \forall i \in S \end{aligned} \quad (9)$$

Note that we consider the benefit of each operator but not each flight because the market shares of operators could be different. The unit-maximum-benefit is defined as the ratio of the benefit of each player over the maximum difference between the objective and a reference point (Charkhgard, Esmaeilbeigi, and Charkhgard 2020), hereafter referred to as the Unit Benefit Ratio (UBR). The UBR ranges from 0 to 1, and a larger value means a higher unit benefit. NSWP with equal weights/powers among different players attempts to make the UBR of each player relatively the same, which is how equity is considered in the NSWP. Take Fig. 6 as an example, where $|S| = 2$ and the power of each player equal to 1 (i.e., $w_1 = w_2 = 1$). The reference point, in this case, is $d = (6, 6)$. NSWP suggests maximizing the benefits of players 1 and 2, which is geometrically to find a Pareto-optimal point so the area between the point and the reference point (6, 6) is maximal. In this case, the Pareto-optimal point (3.5, 4) makes the maximum area from the reference point. With regard to the Pareto-optimal point (3.5, 4), the UBR for player 1 is $\frac{6-3.5}{6-0.5} = 0.45$ and is $\frac{6-4}{6-1} = 0.4$ for player 2, where 0.5 and 1 are the lowest values for players 1 and 2, respectively, among all Pareto-optimal values. The UBRs of the two players at the Pareto-optimal point (3.5, 4) are the closest compared to other pairs of UBRs calculated from other Pareto-optimal points.

Based on NSWP, a multiplication model is introduced to consider fairness among different operators. Although the objective function is different from the summation model, the constraints are identical to the summation model to ensure conflict-free operations. Since the feasible region is not continuous, there is no guarantee that the fairness measure (UBR) will always be equal, but it guarantees that there are no other solutions that would create better fairness among operators. For introducing the multiplication model, several new notations are introduced as follows:

$O : (o_1, \dots, o_p)$: set of operators

$d_f = \max c_f^h, \forall h \in L^f$: maximal flying cost of flight f taking all allowed flight levels

$d_o = \sum_{f \in o} d_f, \forall o \in O$: maximal cost of an operator

Equity can be modeled for either each flight or each operator, and the term “players” used in the general form is equivalent to flights or operators in the multiplication model. When modeling equity for each flight, the objective is to maximize the product of each flight's benefit, which is the difference between the reference point d_f and the actual cost $C_f^h \phi_h^f$, as shown in Equation (11). It should be noted that the worst-case scenario cost d_f of the flight is used as the approximation of the reference point. When modeling equity among operators, the objective is to maximize the product of each operator's benefit, which is the difference between the reference point d_o and actual cost $\sum_{f \in o} C_f^h \phi_h^f$. Similarly, the worst-case scenario cost of each operator is used as the approximation of the reference point. Also, operators may negotiate for premier service (i.e., higher w in multiplication model [9]) by paying a higher service fee. However, in this study, we assumed that weight w is 1 for all operators. Thus, w is omitted in the following equations:

$$\text{Max} \prod_{f \in F} (d_f - C_f^h \phi_h^f) \quad (10)$$

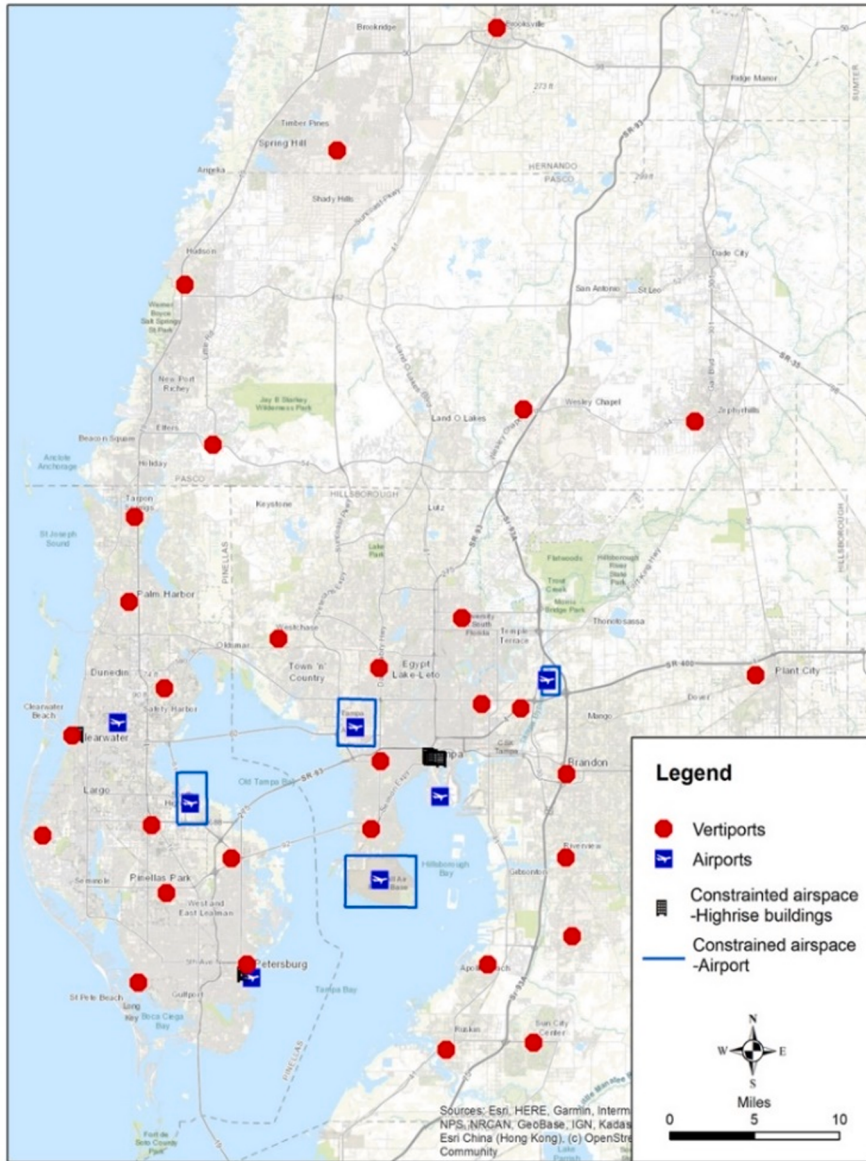


Fig. 7. Airports, vertiport locations, and restricted airspaces in Tampa Bay.

$$\text{Max} \prod_{o \in O} (d_o - \sum_{f \in o} C_f^h \phi_h^f) \quad (11)$$

3.2.3. Solution algorithms

The summation model is formulated as an integer program and can be solved by any commercial solver. To solve the multiplication model, we reformulate it as a mixed-integer Second-Order Cone Program (SOCP), a convex programming model that has second-order constraints and can be solved effectively by commercial solvers such as IBM ILOG CPLEX, Gurobi, and FICO Xpress. Although some other approaches have been developed recently to solve this problem, according to one of the coauthors' previous work (Saghand and Charkhgard, 2019), the SOCP reformulation approach has shown to be competitive with other approaches. This reformulation, introduced by Ben-Tal and Nemirovski (1999), optimizes the geometric mean of multiplied terms. That is, the objective function of the model with different operators changes as follows:

$$\max_y \quad (12)$$

Table 1
Tampa Bay area case study settings.

True airspeed for cruise	130 knots
Rate of climb/rate of descent	1000 fpm
Number of vertiports	30
Minimum separation	0.3NM
Number of flight levels	10 (100 ft vertical separation of 500–1400 ft)

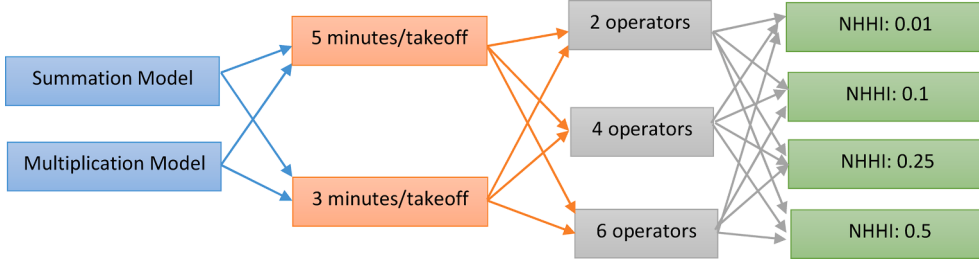


Fig. 8. Experiment design of case study.

$$\text{s.t. } 0 \leq \gamma \leq \left(\prod_{o \in O} \left(d_o - \sum_{f \in o} C_f^h \phi_h^f \right) \right)^{\frac{1}{|O|}} \quad (13)$$

Given γ^* is the optimal solution to this problem, $\gamma^{|O|}$ will be the optimal value of the objective function (12). Constraint (13) can be reduced to a set of second-order constraints. Given k is the smallest value that satisfies $2^k \geq |O|$, Constraint (13) is replaced with the following constraints:

$$0 \leq \gamma \leq \Gamma \quad (14)$$

$$0 \leq \Gamma \leq \sqrt{\tau_{1,k-1} \tau_{2,k-1}} \quad (15)$$

$$0 \leq \tau_{j,l} \leq \sqrt{\tau_{2j-1,l-1} \tau_{2j,l-1}}, \forall j = 1, \dots, 2^{k-1}, l = 1, \dots, k-1 \quad (16)$$

$$0 \leq \tau_{j,0} = d_o - \sum_{f \in o} C_f^h \phi_h^f, \forall j = 1, \dots, |O| \quad (17)$$

$$0 \leq \tau_{j,0} = \Gamma, \forall j = |O| + 1, \dots, 2^k \quad (18)$$

Where Γ and $\tau_{j,l}, \forall j = 1, \dots, 2^k, \forall l = 0, \dots, k-1$ are intermediate variables to handle this reformulation.

4. Case study

A case study of UAM in the Tampa Bay area in Florida was conducted. The locations of 30 vertiports in this area were determined by the study of (Wu and Zhang 2021) titled “Integrated Network Design and Demand Estimation of On-Demand Urban Air Mobility”. In their study, based on simulated disaggregate travel demand data of the Tampa Bay area, the optimal locations of the vertiports were determined to achieve a minimal total generalized cost with consideration of the interactions between vertiports locations and traveler mode choice.

The airspace for the study area was configured with 10 flight levels of 500–1400 ft with a vertical separation of 100 ft. There are seven airports in this area. In this study, restricted airspace was set for each airport that keeps UAM flights from entering the restricted airspaces. In addition, high buildings in downtown Tampa, downtown St. Petersburg, and downtown Clearwater are clustered and defined as different sizes of cuboids from the surface to the layer that covers the tallest building in the cluster. An eVTOL first climbs vertically from the departure vertiport to the assigned flight level, then cruises horizontally at this flight level until it reaches the destination vertiport and starts to descend. The true airspeed of the cruise of eVTOL was set to 130 knots, and the rate of climb/descent was 1000 ft/min. Fig. 7 shows the airports, vertiport locations, and restricted airspaces in the case study. The 3D information of buildings in Tampa Bay was extracted from LiDAR data that was acquired from the 2007 Florida Division of Emergency Management (FDEM) LiDAR Project: Southwest Florida (OCM Partners 2020). The case study settings are shown in Table 1.

Following the steps of LAMS introduced in Section 3.1, given the vertiport locations and 3D information extracted from LiDAR data, the flyable airspace of the case study area was determined. Then, a visibility graph was constructed, and the shortest path (trajectory) of any vertiport pair at each flight level was obtained. Path intersection information was generated and stored in the database together with the shortest paths at each flight level. Then, given simulated flight operation requests, LTMS was applied to generate conflict-free

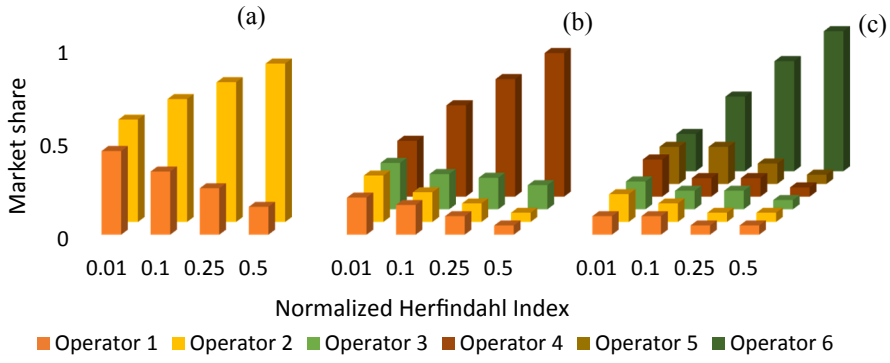


Fig. 9. Market shares by Normalized Herfindahl Index in two-operator, four-operator, and six-operator markets.

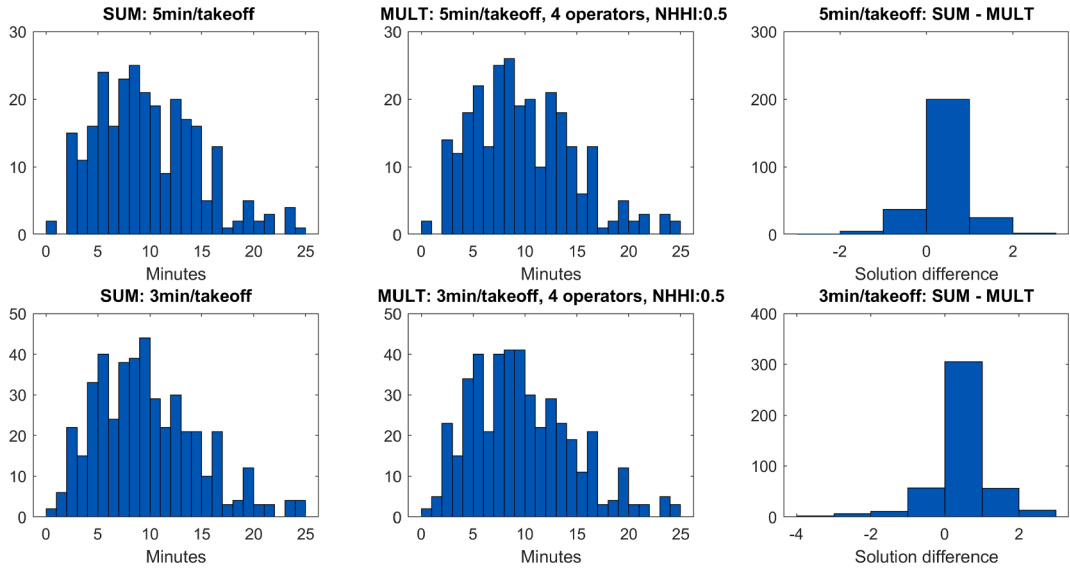


Fig. 10. Comparison of flying time distributions between summation and multiplication models.

trajectories for all flights by solving two mathematical models (summation and multiplication).

4.1. Experiment design

The experiment design was performed to simulate flight operation requests (see Fig. 8); specifically, it considers different operational frequencies, the number of operators, and market concentrations.

Two operational densities (5 min per takeoff and 3 min per takeoff) were designed, i.e., 5 min/takeoff represents every 5 min there is a flight departing from each of the 30 vertiports to a randomly assigned destination, and the departure time is not fixed but generated assuming a uniform distribution in a 2-minute window. Thus, for a 45-min experiment, there will be a total of 270 flights and 450 flights for a density of 5 min/takeoff and a density of 3 min/takeoff, respectively. The experiment design also assumes that two, four, or six operators will use the AAFPS service. In addition, four levels of market concentration indicated with the normalized Herfindahl-Hirschman Index (NHHI) were assumed, which are used to measure the competitiveness of the market. NHHI is computed as:

$$H^* = \frac{(H - 1/N)}{1 - 1/N} \text{ if } N > 1 \\ H^* = 1 \text{ if } N = 1 \quad (19)$$

Where N is the number of firms and H is the Herfindahl-Hirschman Index computed as $H = \sum_{i=1}^N s_i^2$, where s_i is the market share of firm i . NHHI ranges from 0 to 1 and is equal to 0 if all firms have the same market share. A higher NHHI indicates a less equal market share and vice versa. Four levels of NHHI defined in this study were 0.01, 0.1, 0.25, and 0.5. The specific market share of each operator was assumed and is shown in Fig. 9. An NHHI of 0.01 was used to represent a market with a similar share among operators because it is

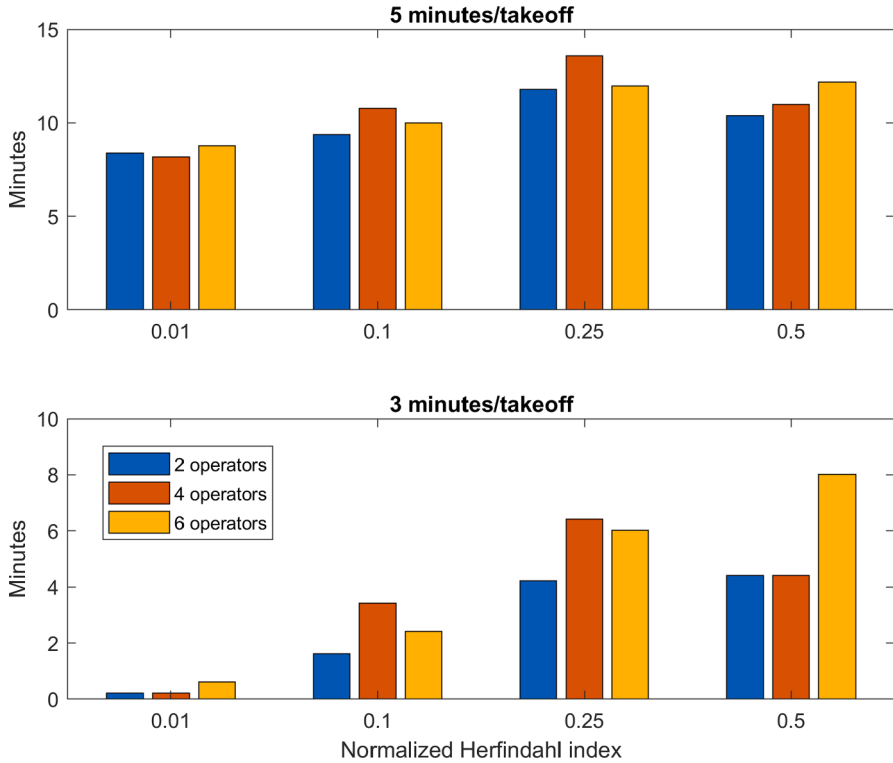


Fig. 11. The difference of optimized system cost between multiplication model and summation model.

impractical to have a strictly equal share among operators. As the NHHI increases, one operator takes more of the market share than others, and NHHI reaches 0.5 when one operator predominantly (occupying over 75% of the market) takes the market.

4.2. Experiment results

The summation model was solved by Gurobi and the multiplication model was solved by reformulating the model into a mixed-integer Second-Order Cone Program (SOCP) and then solved by CPLEX 12.10 on a PC with Core i7-4790 CPU 3.6 GHz 16 GB RAM. For the experiments in the case study, both models were solved to optimality and returned 4D conflict-free trajectories. It should be noted that regardless of the number of operators and market concentrations (not operation frequency), the optimal solutions for the summation model without considering equity among operators did not change because the objective function was to minimize the total flying cost of flights and it did not matter which operator the flights belong to. However, for the multiplication model, different scenarios resulted in different optimal solutions.

Given the optimal solutions, the flying time for each vertiport pair was calculated. Results revealed that the flying time distributions were very similar between the summation model and the multiplication model under different experiment scenarios, as was the average flying time. For instance, Fig. 10 shows the comparison of flying time distributions of the summation model and the multiplication model for one scenario (4 operators, NHHI equal to 0.5) under different operational densities. For the summation model, the flying time distributions were the same under the same operational density. The average flying time from the multiplication model with 3 min/takeoff, 4 operators, and NHHI equal to 0.5 was 9.74 min, and the average flying time was 9.73 min for the summation model under the same setting.

In terms of the solutions, while a large portion of flights had the same solutions (assigned the same flight level) from two models, some flights were assigned different levels in summation and multiplication models. The rightmost two subplots in Fig. 10 show the histogram of solution difference calculated by subtracting the flight levels obtained from the multiplication model from the summation mode. Note that the route network constructed in the case study was a relatively less complex network, where the major impacts of different solutions were acting on the climbing and descending phases of the trip. Nevertheless, the climbing and descending only occupied a very small part of the whole trip in the experiments. For instance, given the rate of climb 1000 fpm, climbing one flight level (100 feet) only takes 6 s while the average flying time was greater than 9 min for a whole trip. Therefore, different solutions for some flights that climbed or descended one or two more flight levels do not change the total flying time too much. If the models are applied for a more complex network with many obstructions or the flight levels are expanded to higher altitude (e.g. 400–3,000 ft instead of the 400–1,500 feet considered in the case study), it is expected to see more distinctions in the solutions of the two models.

Fig. 11 shows a comparison of system costs between the multiplication and summation models. The overall trend was that the system costs from the multiplication model were higher than those from the summation model, and the differences increased with the

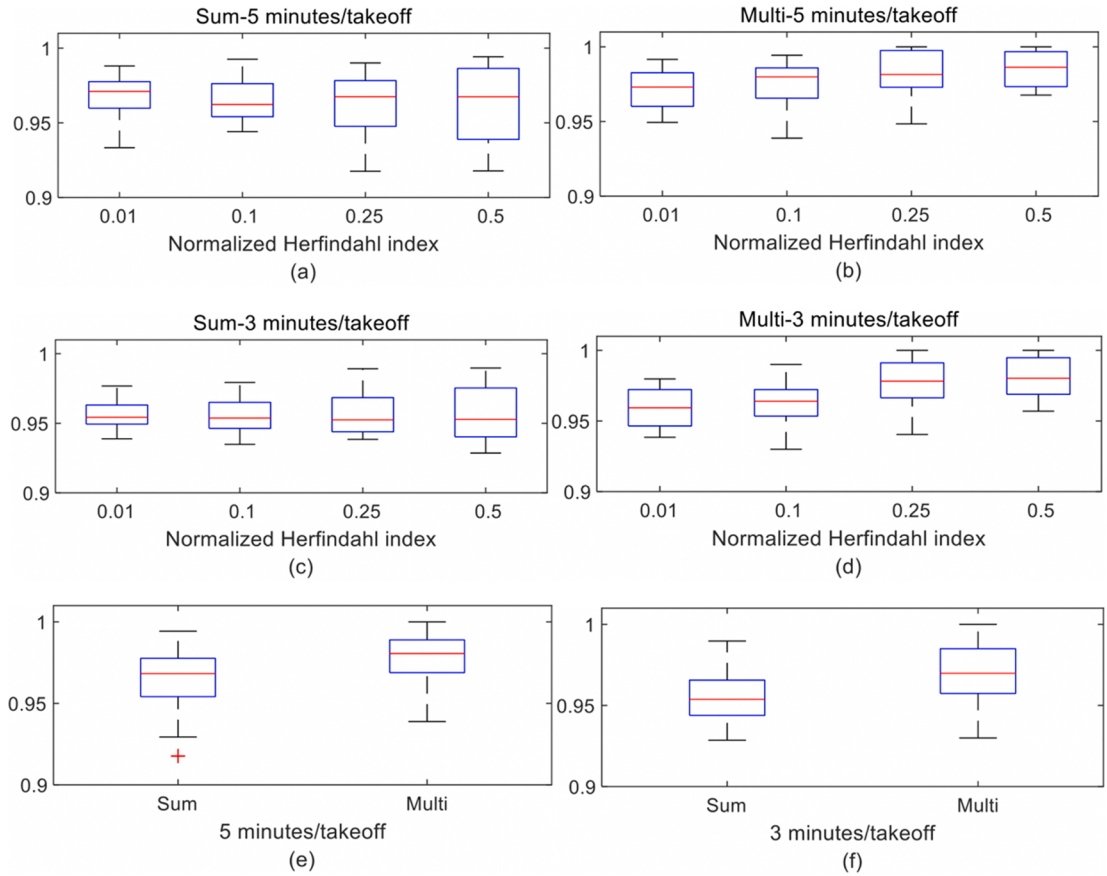


Fig. 12. Unit Benefit Ratio (UBR) by NHHI from summation model and multiplication model.

increase of NHHI indexes. Given that the system cost of the summation model with 5 min/takeoff was 2653 and with 3 min/takeoff was 4380, the difference was no more than 0.5%. Thus, the observation is that system cost is sacrificed for achieving equity among operators. Although the sacrifice is small, it increases when the market is less competitive, and the increasing trend is more significant for operations with higher density.

Statistics for the UBRs of operators are illustrated with boxplots in Fig. 12. Detailed results are included in the appendix in Table 2 through Table 5. Table 2 and Table 3 shows results from the operational density of 5 min per takeoff for the summation model and multiplication model, respectively, and results from the operational density of 3 min per takeoff are shown in Table 4 and Table 5.

It can be seen in Fig. 12(a) and (c) (summation models for different operation densities) that as NHHI increases, the UBR is distributed more widely, which indicates that more unfairness is seen when the market is less competitive. For the multiplication model (Fig. 12b and 12d), the trend is different. Even for a less competitive market (NHHI = 0.5), the variations of UBRs of different operators are small. When comparing the UBR distribution of the summation model vs. the multiplication model for different market concentrations, an upward shift is seen from the multiplication model, which means that the multiplication model improved fairness among operators, especially for a less competitive market when one operator dominates the market. Another observation is that with lower-density operations (Fig. 12e), the UBRs of operators are higher than those in the scenario with higher-density operations (Fig. 12f); however, the fairness improvement is more significant when the operation density is higher.

Fig. 13 shows the computation time comparison. The top chart shows lower operation density with 5 min/takeoff, and the bottom is higher with 3 min/takeoff. The horizontal axis is NHHI. The NHHI does not affect the summation model, so the computation times for different settings are the same. For the multiplication model, the overall trends are that (1) higher-density operations need much longer computation time to solve the problem; (2) more competitive markets (with lower NHHI) need longer computation time; (3) computation time decreases significantly when the NHHI increases; and (4) in scenarios when 75% market share is controlled by one operator, the computation time is almost the same as that of the summation model.

5. Conclusions

Considering the unique challenges of high-density UAM, this study developed an Automated Flight Planning System (AFPS) that can be used to enable Providers of Service for UAM (PSU) for offering airspace management and traffic management services to

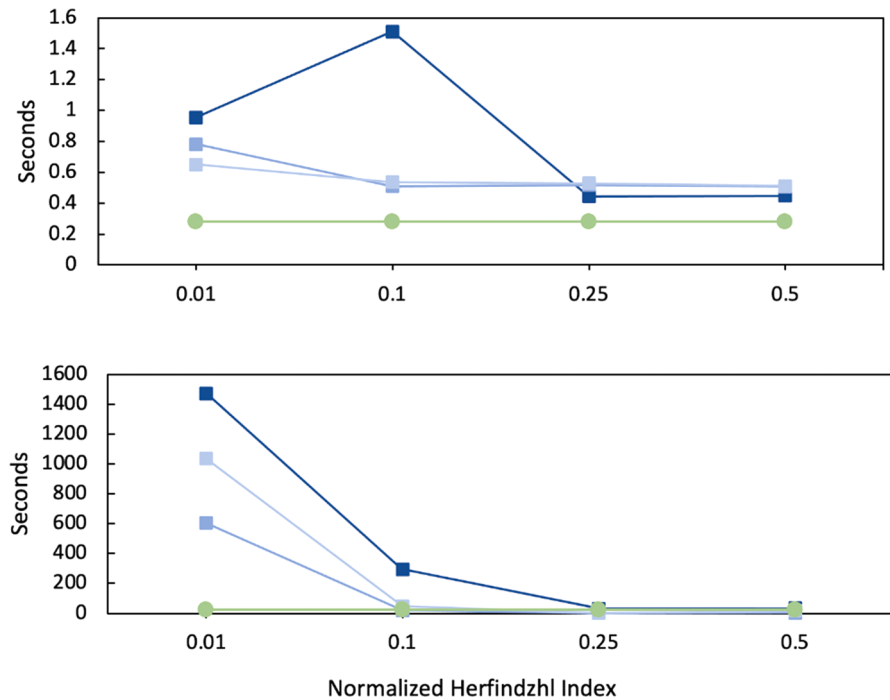


Fig. 13. Computation times by NHHI with the operational density of 5 min/takeoff (top) and 3 min/takeoff (bottom).

Table 2

Summation model: Unit Benefit Ratio (UBR) by Normalized Herfindahl Index with density of 5 min/takeoff.

Summation – 5 min/takeoff				
Normalized Herfindahl Index	0.01	0.1	0.25	0.5
2 operators	0.978	0.993	0.990	0.994
	0.983	0.954	0.970	0.966
4 operators	0.962	0.986	0.990	0.986
	0.972	0.952	0.967	0.987
	0.978	0.954	0.934	0.918
	0.958	0.972	0.931	0.962
6 operators	0.954	0.976	0.984	0.991
	0.968	0.976	0.961	0.929
	0.975	0.944	0.973	0.941
	0.970	0.965	0.965	0.937
	0.988	0.960	0.968	0.974
	0.933	0.955	0.918	0.969

Table 3

Multiplication model: Unit Benefit Ratio (UBR) by Normalized Herfindahl Index with density of 5 min/takeoff.

Multiplication – 5 min/takeoff				
Normalized Herfindahl Index	0.01	0.1	0.25	0.5
2 operators	0.972	0.968	0.974	0.987
	0.992	0.992	1.000	1.000
4 operators	0.974	0.951	0.961	0.968
	0.976	0.978	0.974	0.971
	0.962	0.987	1.000	1.000
	0.960	0.984	0.984	0.994
6 operators	0.954	0.939	0.948	0.972
	0.960	0.963	0.995	0.988
	0.949	0.970	0.979	1.000
	0.983	0.985	0.972	0.986
	0.982	0.982	1.000	0.974
	0.985	0.994	0.990	0.984

Table 4

Summation model: Unit Benefit Ratio (UBR) by Normalized Herfindahl Index with density of 3 min/takeoff.

Summation – 3 min/takeoff				
Normalized Herfindahl Index	0.01	0.1	0.25	0.5
2 operators	0.977	0.979	0.989	0.990
	0.962	0.963	0.950	0.945
4 operators	0.960	0.976	0.980	0.984
	0.950	0.954	0.938	0.965
	0.975	0.937	0.948	0.934
	0.942	0.954	0.955	0.961
6 operators	0.953	0.957	0.973	0.986
	0.955	0.967	0.945	0.943
	0.964	0.951	0.960	0.966
	0.949	0.935	0.963	0.929
	0.950	0.947	0.940	0.943
	0.939	0.946	0.943	0.937

Table 5

Multiplication model: Unit Benefit Ratio (UBR) by Normalized Herfindahl Index with density of 3 min/takeoff.

Multiplication – 3 min/takeoff				
Normalized Herfindahl Index	0.01	0.1	0.25	0.5
2 operators	0.961	0.960	0.966	0.968
	0.980	0.990	0.999	0.998
4 operators	0.945	0.942	0.941	0.965
	0.948	0.961	0.973	0.995
	0.969	0.989	0.991	0.972
	0.977	0.970	0.991	0.995
6 operators	0.948	0.930	0.940	0.957
	0.938	0.955	0.977	0.977
	0.958	0.967	0.980	0.983
	0.943	0.952	0.967	0.969
	0.967	0.973	0.987	0.989
	0.976	0.971	1.000	1.000

multiple UAM operators. Two main components of AFPS are a Low-Altitude Airspace Management System (LAMS), which generates the nodal network of flyable airspace, routing and intersection information for all vertiport pairs, and a Low-Altitude Traffic Management System (LTMS), which detects and resolve potential conflicts of flight operations and generates conflict-free 4D trajectories. Fairness principles are crucial to maintaining a good competitive environment when more entrants enter the UAM market. We have shown that UBR is an appropriate equity indicator that measures the “unit benefit” each operator receives. We demonstrated that for LTMS, by applying Nash Social Welfare Program (the multiplication model), it can maintain fairness for different operators when multiple operators are using the service from one PSU regardless of the market shares and operation patterns of different operators.

The case study of the Tampa Bay area in Florida demonstrated the operability of AFPS and the methodologies used for generating conflict-free 4D trajectories. The multiplication model obtained more equity/fairness (measured by UBR) among operators compared with the summation model, by sacrificing a slight increase in the system cost. The computation time of multiplication models is longer than summation models, but still within seconds for most of the instances.

It is widely recognized that an innovative air traffic service system needs to be constructed to support the emerging UAM. This paper presents exploratory work in this direction. In our ongoing research, more strategies of conflict resolution for flight planning of high-density UAM are proposed, including departure displacement and speed control. Also, we are studying the integration of strategic trajectory planning and tactical conflict resolution to achieve a safe and efficient UAM system by taking uncertainty into consideration. Although we focused on high-density UAM given the unique challenges that UAM with high maturity levels will face, the approach and methodology that we proposed could be used by other types of AAM as well.

In future research, the cost function in the objective function of flight planning could be modified given more understanding of operator business interests and factors influencing their decisions. Also, flight planning needs to take weather patterns into consideration. The Urban Air Mobility (UAM) Market Study report from Booz Allen Hamilton shows that there is limited availability of high-resolution and reliable weather data collected directly in urban areas (Booz Allen Hamilton, 2018). However, by combining available Meteorological Aerodrome Report (METAR), vertical soundings, and pilot reports (PIREP) in several study urban areas, they identified different wind patterns in time of day and seasons. When high resolution and reliable weather data in urban areas becomes available, wind patterns and other historical trends of weather information could be identified and used in the flight planning process. Furthermore, although monitoring the battery level and determining charging schedules of eVTOLs are tactical operational decisions dependent on the charging capacity of each vertiport and flight operational scheduling (distance between origin and destination of succeeding flight), for a future UAM system, a closed-loop framework is needed to take aggregated tactical operational decisions into flight planning for updating constraints in mathematical modeling of determining conflict-free 4D trajectories of high-density UAM

operations.

Declaration of Competing Interest

The authors declare that they have no known competing financial interests or personal relationships that could have appeared to influence the work reported in this paper.

Acknowledgments

The authors gratefully acknowledge the support provided by the Center for Transportation, Environment, and Community Health (CTECH), a University Transportation Center sponsored by the US Department of Transportation through Grant No. 69A3551747119. The contents of this manuscript reflect the views of the authors, who are responsible for the facts and accuracy of the information presented; the contents do not necessarily reflect the official views or policies of the US Department of Transportation.

Appendix

See Tables 2-5.

References

- Allignol, Cyril, Nicolas Barnier, Nicolas Durand, Guido Manfredi, Éric Blond, Dsna Dt, and Maurice Grynogel. 2016. "Integration of UAS in Terminal Control Area." <https://doi.org/10.1109/DASC.2016.7778052>.
- Alonso-Ayuso, A., Escudero, L.F., Javier Martín-Campo, F., 2016. Exact and Approximate Solving of the Aircraft Collision Resolution Problem via Turn Changes. *Transportation Science* 50 (1), 263–274. <https://doi.org/10.1287/trsc.2014.0557>.
- Andrews, John W., Welch, Jerry D., Erzberger, Heinz, 2006. Safety Analysis for Advanced Separation Concepts. *Air Traffic Control Quarterly* 14 (1), 5–24.
- Balakrishnan, Hamsa, and Bala Chandran. 2007. "Efficient and Equitable Departure Scheduling in Real-Time: New Approaches to Old Problems." In 7th USA-Europe Air Traffic Management Research and Development Seminar, pp. 02-05. 2007.
- Barnhart, Cynthia, Bertsimas, Dimitris, Caramanis, Constantine, Fearing, Douglas, 2012. Equitable and Efficient Coordination in Traffic Flow Management. *Transportation science* 46 (2), 262–280. <https://doi.org/10.1287/trsc.1110.0393>.
- Barnier, Nicolas, Allignol, Cyril. 2011. Combining Flight Level Allocation with Ground Holding to Optimize 4D-Deconfliction. ATM Seminar. <https://hal-enac.archives-ouvertes.fr/hal-00938500>.
- Barnier, Nicolas, and Pascal Brisset. 2002. "Graph Coloring for Air Traffic Flow Management," *Annals of operations research* 130, no. 1-4 (2004): 163–78. <https://doi.org/10.1023/B:ANOR.0000032574.01332.98>.
- Ben-Tal, Aharon, Nemirovski, Arkadi, 1999. On Polyhedral Approximations of the Second-Order Cone. *Mathematics of Operations Research* 26 (2), 193–205.
- Bertram, Joshua R, and Peng Wei. 2020. "Distributed Computational Guidance for High-Density Urban Air Mobility with Cooperative and Non-Cooperative Collision Avoidance." In AIAA Scitech 2020 Forum (p. 1371).
- Bertram, J, Wei, P, and Zambreno, J., 2021. "Scalable FastMDP for Pre-departure Airspace Reservation and Strategic De-conflict." In AIAA Scitech 2021 Forum (p. 0779).
- Booz Allen Hamilton, Final Report of Urban Air Mobility (UAM) Market Study, Submitted on Nov. 21, 2018, <https://ntrs.nasa.gov/citations/20190001472>, accessed on Oct. 10, 2020.
- Branzei, Simina, Vasilis Gkatzelis, and Ruta Mehta. 2017. "Nash Social Welfare Approximation for Strategic Agents." In Proceedings of the 2017 ACM Conference on Economics and Computation (pp. 611-628).
- Charkhgard, Hadi, Rasul Esmailbeigi, and Parisa Charkhgard. 2020. "The Magic of Nash Social Welfare in Optimization : Do Not Sum–Just Multiply! ". Preprint.
- Courchelle, Valentin, Daniel Delahaye, Daniel González-Arribas, and Manuel Soler. 2017. "Simulated Annealing for Strategic Traffic Deconfliction by Subliminal Speed Control under Wind Uncertainties." In SID 2017, 7th SESAR Innovation Days.
- de Berg, Mark, Marc van Krevel, Otfried Overmars, and Mark Schwarzkopf. 2000. "Chapter 15: Visibility Graphs." *Computational Geometry*, pp.307-317.
- Durand, N., Alliot, J.M. and Noailles, J., 1996, February. Automatic aircraft conflict resolution using genetic algorithms. In Proceedings of the 1996 ACM symposium on Applied Computing (pp. 289-298).
- Eby, M.S. and Kelly, W.E., 1999, March. Free flight separation assurance using distributed algorithms. In 1999 IEEE Aerospace Conference. Proceedings (Cat. No. 99TH8403) (Vol. 2, pp. 429-441). IEEE.
- Federal Aviation Administration (FAA), 2020. Fact sheet – Small Unmanned Aircraft Systems (UAS) REGULATIONS (Part 107). https://www.faa.gov/news/fact_sheets/news_story.cfm?newsId=22615.
- Frazzoli, E., Mao, Z.H., Oh, J.H., Feron, E., 2001. Resolution of conflicts involving many aircraft via semidefinite programming. *Journal of Guidance, Control, and Dynamics* 24 (1), 79–86.
- Guterres, M., Jones, S., Orrell, G. and Strain, R., 2017. ADS-B surveillance system performance with small UAS at low altitudes. In AIAA Information Systems-AIAA Infotech@ Aerospace (p. 1154).
- Ho, Florence, Geraldes, Ruben, Goncalves, Artur, Cavazza, Marc, Prendinger, Helmut, 2019. Improved Conflict Detection and Resolution for Service UAVs in Shared Airspace. *IEEE Transactions on Vehicular Technology* 68 (2), 1231–1242. <https://doi.org/10.1109/TVT.2018.2889459>.
- Hoekstra, J.M., Van Gent, R.N.H.W., Ruigrok, R.C.J., 2002. Designing for Safety: The 'Free Flight' Air Traffic Management Concept. *Reliability Engineering and System Safety* 75 (2), 215–232. [https://doi.org/10.1016/S0951-8320\(01\)00096-5](https://doi.org/10.1016/S0951-8320(01)00096-5).
- Hunter, George, Peng Wei, and Chris Wargo. 2019. "Service-Oriented Separation Assurance for Small UAS Traffic Management." Integrated Communications, Navigation and Surveillance Conference, ICNS 2019-April: 1–11. <https://doi.org/10.1109/ICNSURV.2019.8735193>.
- Islami, A., Chaimatanan, S., Delahaye, D., 2017. Large-scale 4D trajectory planning. In: *Air Traffic Management and Systems II*. Springer, Tokyo, pp. 27–47.
- Jacquillat, Alexandre, Vaze, Vikrant, 2018. Interairline Equity in Airport Scheduling Interventions. *Transportation Science* 52 (4), 941–964. <https://doi.org/10.1287/trsc.2017.0817>.
- Jardin, Matt R., 2005. Analytical Relationships Between Conflict Counts and Air-Traffic Density. *Journal Of Guidance, Control, and Dynamics* 28 (6). <https://doi.org/10.2514/1.12758>.
- Krozel, Jimmy, Mark Peters, and Karl Bilimoria. 2000. "A Decentralized Control Strategy for Distributed Air/Ground Traffic Separation." In AIAA Guidance, Navigation, and Control Conference and Exhibit. Reston, Virginia: American Institute of Aeronautics and Astronautics. <https://doi.org/10.2514/6.2000-4062>.

- Kuchar, J.K., Yang, L.C., 2000. A review of conflict detection and resolution modeling methods. *IEEE Transactions on intelligent transportation systems* 1 (4), 179–189.
- Logan, M.J., Bird, E., Hernandez, L. and Menard, M., 2020. Operational Considerations of Small UAS in Urban Canyons. In AIAA Scitech 2020 Forum (p. 1483). <https://doi.org/10.2514/6.2020-1483>.
- Lulli, Guglielmo, Odoni, Amedeo, 2007. The European Air Traffic Flow Management Problem. *Transportation Science* 41 (4), 431–443. <https://doi.org/10.1287/trsc.1070.0214>.
- Morgan Stanley. 2019. “Flying Car and Autonomous Aircraft Research | Morgan Stanley.” <https://www.morganstanley.com/ideas/autonomous-aircraft>.
- Nace, Dritan, Jacques Carlier, Linh Doan, and Vu Duong. 2003. “A Linear Programming Approach for Route and Level Flight Assignment.” In 5th EUROCONTROL & FAA ATM R&D Seminar. http://atm2001.eurocontrol.fr/past-seminars/5th-seminar-budapest-hungary-june-2003/papers/paper_094.
- Nash Jr., John F., 1950. *The Bargaining Problem*. *Econometrica: Journal of the Econometric Society* 155–162.
- NASA, Overview of Urban Air Mobility, <https://ntrs.nasa.gov/api/citations/20200000618/downloads/20200000618.pdf>, accessed on Oct. 12, 2020.
- National Academies of Sciences Engineering and Medicine (NASEM). 2020. Advancing Aerial Mobility: A National Blueprint. Advanced Aerial Mobility. <https://doi.org/10.17226/25646>.
- NextGEN. 2020. “UAM ConOps V1.0”.
- Nguyen, Nhan Tam, Nguyen, Trung Thanh, Roos, Magnus, Rothe, Jörg, 2014. Computational Complexity and Approximability of Social Welfare Optimization in Multiagent Resource Allocation. *Autonomous Agents and Multi-Agent Systems* 28 (2), 256–289. <https://doi.org/10.1007/s10458-013-9224-2>.
- OCM Partners. 2020. “2007 Florida Division of Emergency Management (FDEM) Lidar Project: Southwest Florida.” 2020. <https://www.fisheries.noaa.gov/inport/item/49677>.
- Prevot, Thomas, Vernal Battiste, Everett Palmer, and Stephen Shelden. 2003. “Air Traffic Concept Utilizing 4d Trajectories and Airborne Separation Assistance.” In AIAA Guidance, Navigation, and Control Conference and Exhibit (p. 5770). <https://doi.org/10.2514/6.2003-5770>.
- Raghunathan, Arvind U., Gopal, Vipin, Subramanian, Dharmashankar, Biegler, Lorenz T., Samad, Tariq, 2004. Dynamic Optimization Strategies for Three-Dimensional Conflict Resolution of Multiple Aircraft. *Journal of Guidance, Control, and Dynamics* 27 (4), 586–594. <https://doi.org/10.2514/1.11168>.
- Rey, D., Rapine, C., Fondacci, R., El Faouzi, N.E., 2012. Minimization of Potential Air Conflicts through Speed Regulation. *Transportation Research Record* 2300 (1), 59–67. <https://doi.org/10.3141/2300-07>.
- Richards, A. and How, J.P., 2002, May. Aircraft trajectory planning with collision avoidance using mixed integer linear programming. In Proceedings of the 2002 American Control Conference (IEEE Cat. No. CH37301) (Vol. 3, pp. 1936-1941). IEEE.
- Saghand, P. G., and Charkgard, H., 2019, Exact solution approaches for integer linear generalized maximum multiplicative programs through the lens of multi-objective optimization. Preprint http://www.optimization-online.org/DB_HTML/2019/10/7435.html.
- Schouwenaars, T., De Moor, B., Feron, E. and How, J., 2001, September. Mixed integer programming for multi-vehicle path planning. In 2001 European control conference (ECC) (pp. 2603-2608). IEEE.
- SESAR Joint Undertaking, Sustainability, airspace optimization and urban air mobility - focus of latest very large-scale demonstrations, <https://www.sesarju.eu/news/sustainability-capacity-and-urban-air-mobility-focus-newly-launched-sesar-demonstrator-call>, accessed on March. 1, 2021.
- SESAR Joint Undertaking, 2020, Consolidated report on SESAR U-space research and innovation results.
- SESAR Joint Undertaking, 2019, Concept of Operations for U-space.
- Sigurd, K. and How, J., 2003, August. UAV trajectory design using total field collision avoidance. In AIAA Guidance, Navigation, and Control Conference and Exhibit (p. 5728).
- Sunil, E., Hoekstra, J., Ellerbroek, J., Bussink, F., Nieuwenhuizen, D., Vidovavljevic, A., and Kern, S., 2015. “Metropolis: Relating Airspace Structure and Capacity for Extreme Traffic Densities.” ATM seminar 2015, 11th USA/EUROPE Air Traffic Management R&D Seminar, FAA & Eurocontrol, Jun 2015, Lisboa, Portugal.
- Tan, Q., Wang, Z., Ong, Y.S., Low, K.H., 2019. Evolutionary Optimization-Based Mission Planning for UAS Traffic Management (UTM). International Conference on Unmanned Aircraft Systems (ICUAS) 2019, 952–958. <https://doi.org/10.1109/ICUAS.2019.8798078>.
- Thippavong, David P., Rafael Apaza, Bryan Barmore, Vernal Battiste, Barbara Burian, Quang Dao, Michael Feary, et al. 2018. “Urban Air Mobility Airspace Integration Concepts and Considerations.” In 2018 Aviation Technology, Integration, and Operations Conference. Reston, Virginia: American Institute of Aeronautics and Astronautics. <https://doi.org/10.2514/6.2018-3676>.
- Vascik, Parker D., Hamsa Balakrishnan, and R John Hansman. 2018. “Assessment Of Air Traffic Control For Urban Air Mobility and Unmanned Systems.” 8th International Conference on Research in Air Transportation, Castelldefels, Barcelona, Spain: ICRAT.
- Vela, Adan, Senay Solak, William Singhouse, and John Paul Clarke. 2009. “A Mixed Integer Program for Flight-Level Assignment and Speed Control for Conflict Resolution.” Proceedings of the IEEE Conference on Decision and Control, 5219–26. <https://doi.org/10.1109/CDC.2009.5400520>.
- William, C, B Cotton, and David J Wing. 2018. “Airborne Trajectory Management for Urban Air Mobility.” In 2018 Aviation Technology, Integration, and Operations Conference (p. 3674).
- Wu, Z., Zhang, Y., 2021. Integrated Network Design and Demand Estimation of on-Demand Urban Air Mobility. *Engineering* 7 (4), 473–487. <https://doi.org/10.1016/j.eng.2020.11.007>.
- Yang, Xuxi, Lisen Deng, and Peng Wei. 2019. “Multi-Agent Autonomous On-Demand Free Flight Operations in Urban Air Mobility.” In International Conference on Research in Air Transportation (ICRAT), Barcelona, Spain.
- Yang, X., Wei, P., 2020. Scalable Multi-Agent Computational Guidance with Separation Assurance for Autonomous Urban Air Mobility. *Journal of Guidance, Control, and Dynamics* 1–14.
- Zhu, Guodong, and Peng Wei. 2019. “Pre-Departure Planning for Urban Air Mobility Flights with Dynamic Airspace Reservation.” In AIAA Aviation 2019 Forum (p. 3519).